Supplemental material: Material and methods

Assessment of colonoscopy in mice- Animals were anesthetized i.p. with a mixture of 90-120 mg per kg body weight ketamine (Narketan 10 %, Vétoquinol AG, Bern Switzerland) and 8 mg per kg body weight xylazine (Rompun 2 %, Bayer, Lyssach, Switzerland). Animals were examined as described previously (Becker, C. et al., High resolution colonoscopy in live mice. Nat Protoc, 2006. 1(6): p. 2900-4 and Huang, E.H. et al., Colonoscopy in mice. Surg Endosc, 2002. 16(1): p. 22-4). The solid endoscope was introduced per anus with a lubricant (4 % lidocaine) into the sedated mouse. The colon was gently inflated with air. Recording was performed with the Tele Pack Pal 20043020 (Karl Storz Endoskope, Tuttlingen, Germany).

TUNEL- Apoptosis was quantified by TUNEL technology with the In Situ Cell Death Detection Kit (#11684795910, Roche, Mannheim, Germany) as described by the manufacturer. For positive control a section was incubated with DNase I to obtain DNA ends for fluorescent labeling by TUNEL. For negative control a section was incubated without enzyme for end labeling.

Flow cytometry- Cells in suspension were resuspended in 70 % ice cold methanol. Flow cytometry was performed using a Coulter EPICS XLMCL (Coulter, Immunotech, Krefeld, Germany). Fluorescence for fluorescein isothiocyanate was collected at 530 nm. Data analysis was performed using WIN-MDI (facs.scripps.edu).

Western blot- Cells were lysed in sodium dodecyl sulfate polyacrylamide sample buffer (125 mM Tris-HCl (pH 6.8), 4 % (w/v) sodium dodecyl-sulfate polyacrylamide, 20 % (v/v) glycerol, 0.02 % (w/v) bromphenol blue and 50 mM dithiothreitol, added just before use) before sonicated on ice. Western blotting was performed by using NuPAGE Bis-Tris Western gels (Invitrogen). After electrophoresis, proteins were electro-blotted onto nitrocellulose membranes (Hybond ECL, Amersham Biosciences). Membranes were blocked with horse serum, incubated with primary antibody, washed and incubated with horseradish peroxidase-conjugated secondary antibody. The proteins were visualized using enhanced chemiluminescence (ECL) system LumiGLO and exposure to a Hybond ECL film (Amersham Biosciences). Equal loading of the samples was demonstrated by reprobing membranes with an anti-β-actin antibody.

Vectors for BMF knock down- Vectors were cloned as described in the supplement and in [37]. Briefly, constructs for functional analyses were derived from the lentiviral plasmid pHR-SIN-CSGW-_Not, kindly provided by Mary Colins, UK. Vectors for conditional over-expression and RNAi were rendered GATEWAY™-compatible by insertion of AttR-site flanked ccdB-CM cassettes ("DEST" cassette, Invitrogen).

shRNA oligonucleotides for conditional gene knock down were cloned into pENTR-THT. This GATEWAY™-compatible vector contains a tetracycline-sensitive RNAseP H1 promoter (THT) that controls the expression of the shRNA. The THT-shRNA cassette was recombined into a lentiviral RNAi destination vector pHR-Dest-SFFV-eGFP, which was generated by insertion of a destination cassette (rfc-1) into the blunt-ended *Eco*RI site of pHR-SIN-CSGW-_Not.

IEC isolation- Human colonic mucosa from surgical specimens was cut into small strips. Mucus was removed by incubation for 30 min at room temperature in 1 mM DTT (Sigma, Taufkirchen, Germany) in 50 ml Hanks' balanced salt solution (HBSS, PAA, Linz, Austria). Mucosal strips were incubated in 1 mM EDTA (Sigma) for 10 min at 37°C. Tubes were shaken vigorously 5 to 10 times. Mucosal strips were removed by passing the slurry over a coarse mesh (400 µm, Carl Roth GmbH, Karlsruhe, Germany) and IEC were purified using a mesh filter (80 µm, Sefar, Kansas City, USA). The suspension containing the IEC crypts was passed over the filter and intact IEC crypts were eluted by inverting the filter in culture medium.

RNA isolation and PCR- Total RNA was prepared from tissue samples using RNeasy® kit (Qiagen, Hilden, Germany) and reverse transcribed (Promega, Madison, WI, USA). Integrity of mRNA was determined with the Agilent 2100 bioanalyzer and mRNA with a RIN > 8 was used. Amplicons are: upstream: 5´-GTGGCAACATCAAGCAGAGGTA-3´,

downstream: 5´-CGGTGGAACTGGTCTGCAA–3, probe 5´-6-FAM-AGATTGCCCGAAAGCTTC AGTGC-TAMRA (6-carboxy-tetramethyl-rhodamine)-3´ designed using Primer Express 1.5 (Applied Biosystems, CA, USA). Oligonucleotides for GAPDH were from ABI. Reaction mix: Universal Master Mix (Applied Biosystems), forward/reverse primer 750 nM, probe 250 nM, template 50 ng/well. Reactions were performed in triplicate using the ABI PRISM® 7700 Sequence Detection System (Applied Biosystems) at 50°C for 2 min, 95°C for 10 min, followed by 40 cycles of 95°C for 15 sec and 60°C for 1 min.
PCR for detection of p*BMF*-RNAi were performed in a TRIO-Thermoblock (Biometra, Goettingen, Germany): attB1: 5´-ACAAGTTTGTACAAAAAAGCAGGCT-3´, attB2: 5´-ACCACTTTGTACAAGAAAGCTGGGT-3´. PCR for attB comprised 25 cycles: 94°C for 30 sec, 55°C for 30 sec, 72°C for 30 sec.

The amount of reporter dye fluorescence was monitored using Sequence Detector Software (SDS version 2.1, PE Applied Biosystems). Fluorescence values of *GAPDH* were subtracted from those of *BMF* and relative *BMF* gene expression was calculated using the ddCt method.

Virus generation and Transfection

Lentiviral packaging plasmid pCMV 8.91, the plasmid encoding the viral envelope protein pMD-G and the plasmid encoding for the shRNA pHR-THT-BMFI human-PURO were described previously [36] or kindly provided Didier Trono, Lausanne, Switzerland. HEK293T cells were transfected with LipofectAMINE (#18324-111, Invitrogen life technologies, CA, USA). Plates were shifted to 32°C to allow optimal packaging. After 24, 48, 72 and 96 h, supernatants were filtered through a 0.22 μm mesh. PCR was performed to control development of virus (supplemental figure 3A). An eGFP cassette allowed flow cytometrical control of transfection efficiency. Efficient transfection of NIH3T3 cells was examined after 3 days. 95.6% of the transfected cells were GFP positive (black graph, supplemental figure 3B) compared to mock-transfected cells (white graph). Downregulation of BMF protein following knock down of *BMF* was confirmed by Western in CCRF-CEM-C7H2 cells [36].

Supplemental material: Table

Patients recruited from the University of Regensburg							
	gender	**age**	**disease**	**disease behavior**	**used for**	**figure**	**Basis**
1	m	64	sigmoid carcinoma	no inflammation	real-time PCR	2D, E / 3A	tissue
2	m	62	sigmoid carcinoma	no inflammation	real-time PCR	2D, E / 3A	tissue
3	f	59	sigmoid carcinoma	no inflammation	real-time PCR	2D, E / 3A	tissue
4	m	32	sigmoid carcinoma	no inflammation	immunofluorescence / western / real-time PCR	2D, E / 3A, B	tissue
5	f	32	Crohn's disease	no inflammation	immunofluorescence / western / real-time PCR	2D, E / 3A, B	tissue
6	f	70	sigmoid carcinoma	no inflammation	immunofluorescence / western / real-time PCR	3A, B	tissue
7	m	23	sigmoid diverticulosis	severe inflammation	real-time PCR / DAPI staining	3A / 4D, E, F	tissue
8	f	36	Crohn's disease	no inflammation	real-time PCR / DAPI staining	2D, E / 3A / 4D, E, F	tissue
9	m	64	sigmoid carcinoma	no inflammation	real-time PCR / DAPI staining	3A / 4D, E, F	tissue
10	m	62	sigmoid carcinoma	no inflammation	real-time PCR / knock down	3A	tissue
11	f	70	sigmoid carcinoma	no inflammation	real-time PCR / knock down	3A	tissue
12	f	53	Crohn's disease	no inflammation	real-time PCR / knock down	2D, E / 3A	tissue
13	m	61	sigmoid carcinoma	no inflammation	real-time PCR / knock down	3A, 5C	tissue
14	m	58	sigmoid carcinoma	no inflammation	real-time PCR / knock down	3A, 5C	tissue
15	f	74	sigmoid carcinoma	no inflammation	real-time PCR / knock down	3A, 5C	tissue
16	f	33	Crohn's disease	no inflammation	real-time PCR / knock down	3A, 5C	tissue
17	m	66	sigmoid carcinoma	no inflammation	real-time PCR / knock down	3A, 5C	tissue
18	m	19	Crohn's disease	mild inflammation	real-time PCR / knock down	3A, 5C	tissue
19	m	73	Crohn's disease	mild inflammation	real-time PCR / immunohistochemistry	3A	tissue
20	m	17	Crohn's disease	mild inflammation	immunohistochemistry	not shown	tissue
21	f	50	sigmoid diverticulosis	no inflammation	immunohistochemistry	not shown	tissue
22	m	54	sigmoid carcinoma	no inflammation	immunohistochemistry	not shown	tissue
23	m	24	Crohn's disease, stenosis	mild inflammation	immunohistochemistry	not shown	tissue
24	f	49	Crohn's disease	no inflammation / severe inflammation	immunohistochemistry	not shown	2 x tissue
25	f	33	Crohn's disease		immunohistochemistry	not shown	tissue
26	m	74	sigmoid diverticulosis	no inflammation	immunohistochemistry	not shown	tissue
27	f	43	Crohn's disease	no inflammation / mild inflammation	immunohistochemistry	not shown	2 x tissue
28	f	53	sigmoid diverticulosis	mild inflammation	immunohistochemistry	not shown	tissue
29	f	48	sigmoid diverticulosis	no inflammation	immunohistochemistry	not shown	tissue
30	m	66	Crohn's disease, fistula	no inflammation / severe inflammation	immunohistochemistry	not shown	2 x tissue
31	f	47	Crohn's disease, carcinoma	mild inflammation	immunohistochemistry	not shown	tissue
32	f	23	Crohn's disease, stenosis	mild inflammation	immunohistochemistry	not shown	tissue
33	f	28	Crohn's disease, stenosis	no inflammation	immunohistochemistry	2A, B	tissue
34	m	36	carcinoma	no inflammation / severe inflammation	immunohistochemistry	not shown	2 x tissue
35	f	34	sigmoid carcinoma	no inflammation	immunohistochemistry	not shown	tissue
36	f	36	Crohn's disease, carcinoma	severe inflammation	immunohistochemistry	not shown	tissue
37	m	53	sigmoid carcinoma	no inflammation	immunohistochemistry	not shown	tissue
37	f	49	sigmoid carcinoma	no inflammation	immunohistochemistry	not shown	tissue
38	m	36	Crohn's disease	no inflammation	immunohistochemistry	2C	tissue
39	f	41	Crohn's disease, stenosis	no inflammation	immunohistochemistry	not shown	tissue
40	m	38	Crohn's disease, stenosis	mild inflammation	immunohistochemistry	not shown	tissue
41	f	52	sigmoid carcinoma	no inflammation	immunohistochemistry	not shown	tissue

Patients recruited from the University of Zurich							
	gender	**age**	**disease**	**disease behavior**	**used for**	**figure**	**Basis**
42	m	31	Crohn's disease	mild inflammation	real-time PCR / knock down	S2A, B	tissue
43	m	42	ulcerative colitis	mild inflammation	real-time PCR / knock down	S2B	tissue
44	m	56	carcinoma	no inflammation	real-time PCR / knock down	4A, B, C / S2A	tissue
45	f	68	sigmoid diverticulosis	no inflammation	real-time PCR / knock down	4A, B, C / S2A	tissue
46	m	89	carcinoma	no inflammation	real-time PCR / knock down	4A, B, C / S2A	tissue
47	m	66	sigmoid carcinoma	no inflammation	real-time PCR / knock down	S2A	tissue
48	f	80	carcinoma	no inflammation	real-time PCR / knock down	S2A	tissue
49	m	78	carcinoma	no inflammation	real-time PCR / knock down	S2A	tissue
50	f	76	sigmoid diverticulitis	mild inflammation	real-time PCR / knock down	S3	tissue
51	m	62	carcinoma	no inflammation	real-time PCR / knock down	S2A	tissue
52	m	64	carcinoma	no inflammation	real-time PCR / knock down	S2A, B	tissue
53	m	50	Crohn's disease	mild inflammation	real-time PCR / knock down	S2B	tissue
54	m	38	carcinoma	no inflammation	real-time PCR / knock down	5A, B, C, D / S2A	tissue
55	m	53	carcinoma	no inflammation	real-time PCR / knock down	5A, B, C, D / S2B	tissue
56	m	30	Crohn's disease, fistula	no inflammation	real-time PCR / knock down	5A, B, C, D	tissue
57	w	61	carcinoid	no inflammation	real-time PCR / knock down	S2B / S3	tissue
58	w	75	adenoma	no inflammation	real-time PCR / knock down	S2B / S3	tissue
59	f	59	autoimmune colitis / carcinoma / diverticulitis	severe inflammation	real-time PCR / knock down	S3	tissue
60	m	38	ulcerative colitis	severe inflammation	real-time PCR / knock down	S3	tissue
61	f	56	sigmoid volvolus	no inflammation	real-time PCR / knock down	S2B / S3	tissue
62	f	64	carcinoid	no inflammation	real-time PCR / knock down	S2B / S3	tissue

Table. Specimens. 29 patients with carcinoma; 7 patients with diverticulosis or diverticulitis; 21 patients with Crohn's disease, two patients with ulcerative colitis, one patient with a sigmoid volvolus, one patient with autoimmune colitis and one patient with both Crohn's disease and carcinoma. Of a total of 62 subjects, 34 were male and 28 were female. Patients were between 17 and 89 years of age (51 ± 17).

Supplemental material: Figures and figure legends

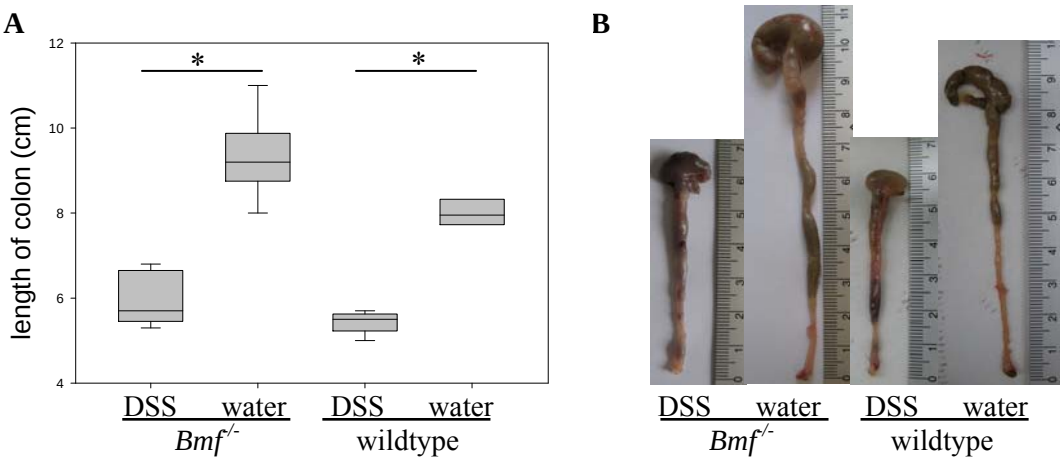

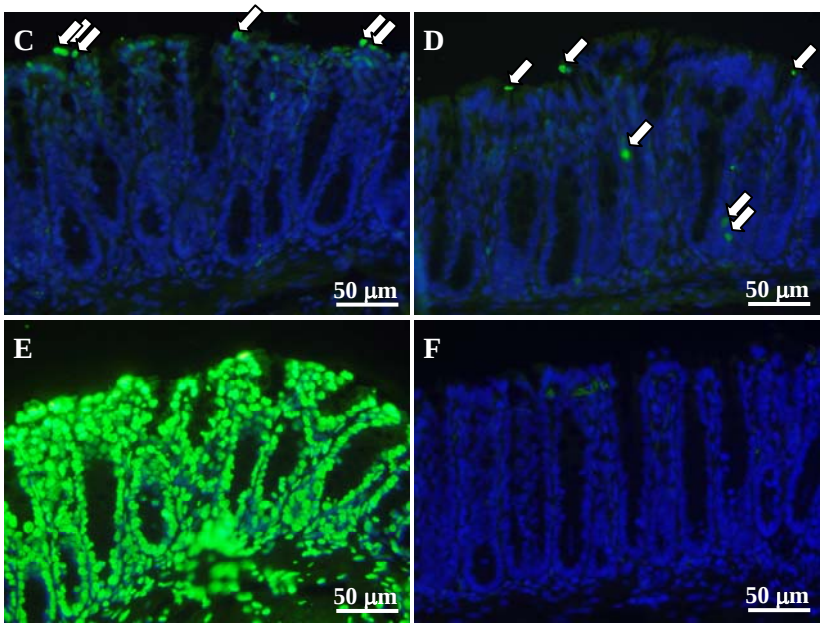

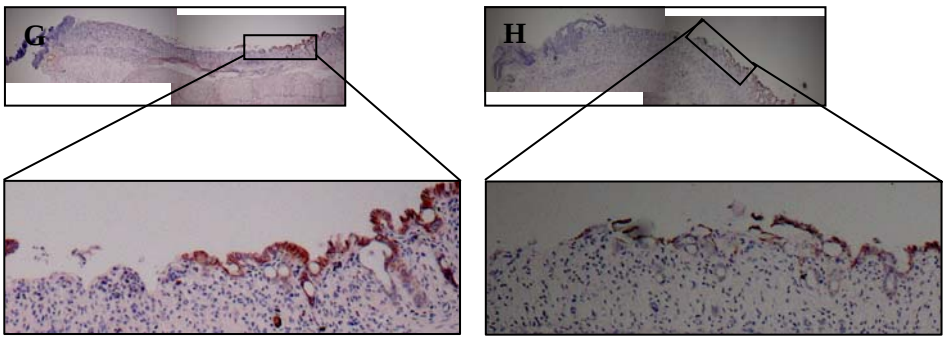

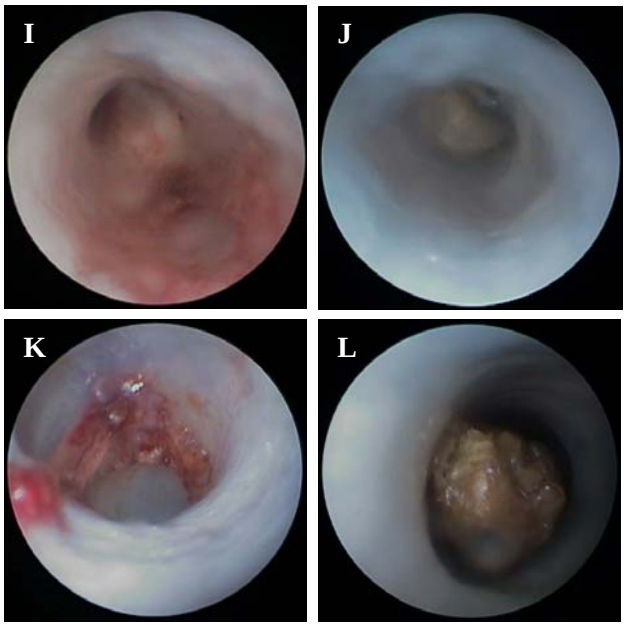

Supplemental figure 1. Colon length, TUNEL, EpCAM staining and colonoscopy. *Bmf*$^{-/-}$ and wildtype received either DSS or water. (A and B) Induction of colitis was followed by a significant reduction of the colon length (five mice each, median shown, One-Way ANOVA, $p < 0.05$ (*)). *Bmf*$^{-/-}$ with and without colitis showed an increased colon length compared to wildtype (images representative for five mice each). TUNEL staining and fluorescent DAPI staining of nuclei from (C) *Bmf*$^{-/-}$ and (D) wildtype revealed no difference in cell death from colonic IEC (images representative for five mice each). (E) For positive control a section was incubated with DNase I to obtain DNA ends. (F) For negative control a section was incubated without enzyme for end labeling. EpCAM staining for (G) *Bmf*$^{-/-}$ and (H) wildtype displayed more IEC in DSS treated *Bmf*$^{-/-}$ (images representative for five mice each). Colonoscopy for (I) *Bmf*$^{-/-}$ receiving DSS and (J) water. Colonoscopy for (K) wildtype receiving DSS and (L) water (n = 1 each).

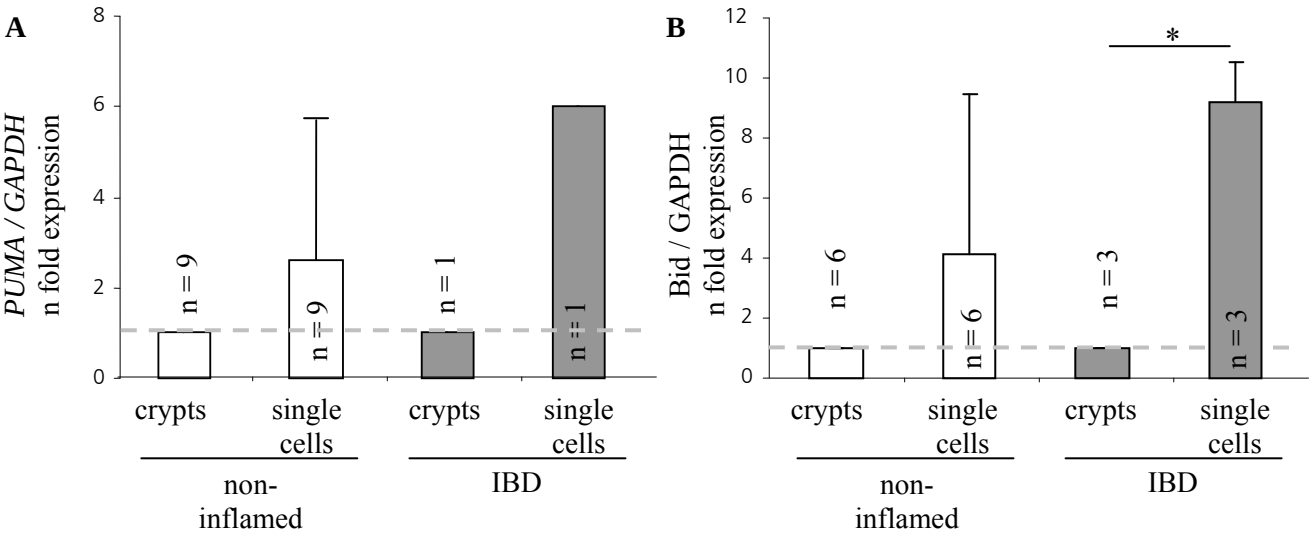

Supplemental figure 2: PUMA and BID mRNA in single cells was significantly increased compared to crypts. (A) PUMA is upregulated in single IEC compared to crypts. (B) BID is significantly increased in single IEC from IBD patients compared to crypts. One-Way ANOVA test was used. * $P < 0.05$.

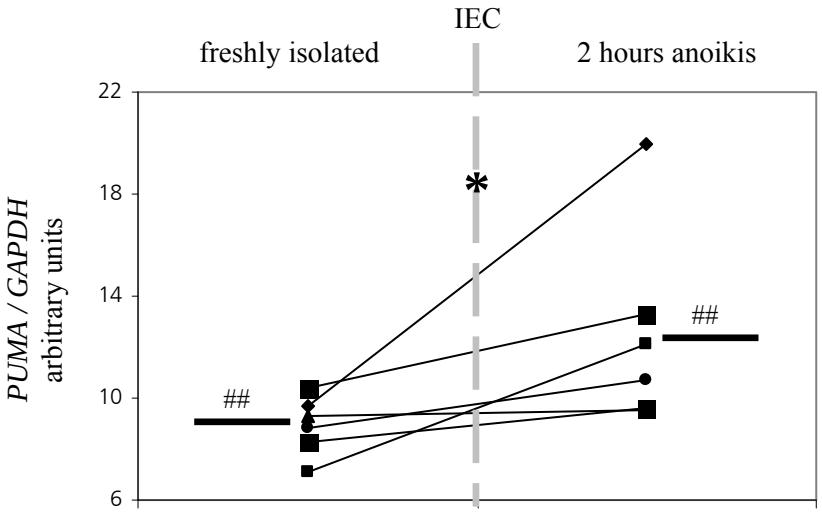

Supplemental figure 3: The initiation of anoikis is followed by a significant upregulation of PUMA mRNA. PUMA real time PCR of freshly isolated human IEC and human IEC 2 hours after *ex-vivo* isolation. A Mann-Whitney Rank Sum Test was performed. $P < 0.05$. n=6, ## = median.

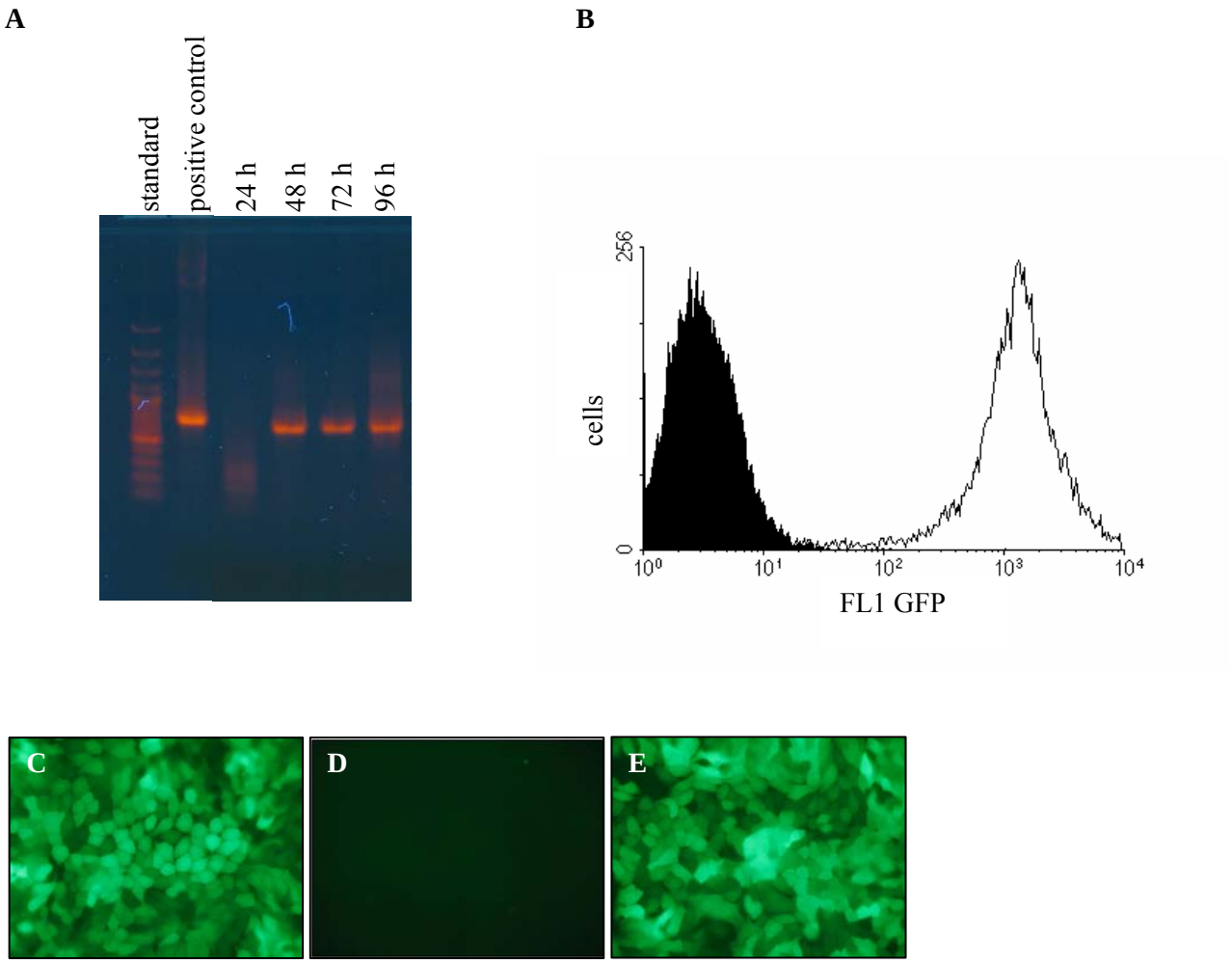

Supplemental figure 4. Lentiviral system for the knock down of *BMF*. HEK293T were transfected with pCMV 8.91, pMD-G and pHR-THT-BMF human-PURO for virus assembly. (A) PCR from supernatant of transfected HEK293. (B) The pHR-THT-BMF vector contains an eGFP cassette. This allowed flow cytometrical control of transfection efficiency in NIH3T3 (white = lentiviral construct with pHR-THT-BMF including eGFP cassette, black = lentiviral construct without eGFP cassette). Efficient transduction of NIH3T3 cells was confirmed flow cytometrically after 3 days. 95.6% of the transduced cells were GFP positive. (C - E) Virus containing supernatants of HEK293 were filtered and used for infection of HT-29. Efficient infection of HT-29 cells was confirmed by fluorescence microscopy after 3 days. HT-29 incubated with the lentivirus-containing supernatant from HEK293 (C), HT-29 incubated with supernatant from HEK293 not containing any lentivirus (D) and HT-29 incubated with mock control (virus with eGFP cassette but without RNAi mediated knock down of *BMF*)-containing supernatant from HEK293 (E). Downregulation of BMF following knock down of *BMF* using these constructs was also confirmed by Western in CCRF-CEM-C7H2 cells [36].